www.czasopisma.pan.pl PAN POLSKA AKADEMIA NAUK www.journals.pan.pl

Arch. Metall. Mater. **65** (2020), 1, 479-484

DOI: 10.24425/amm.2020.131750

M. SOZAŃSKA[1*], A. MOŚCICKI[2], B. CHMIELA[1]

CHARACTERIZATION OF CORROSION AND STRESS CORROSION CRACKING OF AE44 MAGNESIUM ALLOY

The paper presents the susceptibility of AE44 magnesium alloy to electrochemical corrosion and *stress corrosion cracking* (SCC). The evaluation of the intensity of the interaction of the corrosive environment was carried out using the corrosion tests and the *Slow Strain Rate Test* (SSRT). Corrosion tests performed in 0.1 M Na_2SO_4 solution (immersion in solution and under cathodic polarization conditions) revealed that the layer of corrosion products was much thicker after immersion test. The results of SSRT showed that the AE44 alloy deformed in the solution was characterized by higher plasticity compared to the alloy deformed in the air after immersion in solution. Moreover, the fractures were characterized by different morphology. In the case of an alloy deformed in the solution under cathodic polarization many microcracks on the fracture were observed, which were not observed in the case of the alloy deformed in the air.

Keywords: magnesium alloy, fractography, stress corrosion cracking (SCC), AE44

1. Introduction

Magnesium alloys are characterized by poor corrosion resistance, what limits their wide application [1-4]. There are two main reasons of poor corrosion resistance [5]: (i) oxide and hydroxide layer on the alloy surface do not protect against the environment and (ii) precipitates of secondary phases and impurities may lead to galvanic corrosion. The main phenomena associated with the electrochemical corrosion is oxidation of metal ($M \rightarrow M^{+} + e^{-}$), releasing of the atomic hydrogen (during the contact with the electrolyte and cathodic protection) and its adsorption on metal surface [6-11]: ($H_3O^{+} + M + e^{-} \rightarrow MH_{ads} + H_2O$ or $H_2O + M + e^{-} \rightarrow MH_{ads} + OH^{-}$). The next stage is absorption of atomic hydrogen ($MH_{ads} \rightarrow MH_{abs}$). When the alloy is mechanically loaded, the absorbed hydrogen leads to stress corrosion cracking (SCC) [12-26]. The occurrence of hydrogen in the structure of magnesium and its alloys has a negative effect. In general, hydrogen leads to classical, unfavorable changes in the microstructure and properties of magnesium alloys exposed to hydrogen, such as decrease in their strength or plastic properties. So far, literature data on stress corrosion cracking are most often devoted commonly used alloys from the Mg-Al and Mg-Al-Zn systems. Rare earth elements (RE) are used as an additive to magnesium alloys to improve their strength properties at elevated temperatures. Also they improve their castability and corrosion resistance. Literature data dedicated to the SCC of magnesium alloys containing RE are rare. In addition, among the available works occur contradictory information. Some literature data confirms the beneficial effect of the additive of RE on the resistance of magnesium alloys to SCC, while other authors report their high susceptibility to SCC [23-26]. Therefore, detailed investigations that can determine the susceptibility of magnesium alloys with RE to SCC seems necessary.

2. Material and methodology

The research material was AE44 casting magnesium alloy containing rare earth elements (RE). The chemical composition of the alloy was as follows (wt. %): 4.2 Al, 0.2 Mn, 0.1 Si, 4.2 RE, Mg – balance. The material was manufactured by die-casting method in a form of bars (12 mm in diameter).

The experiment consisted of two basic stages:

1. Analyzes morphology, chemical and phase composition of corrosion products (without mechanical loads),
2. Morphology of fracture surface in conditions stress corrosion cracking (SSC) analysis.

In the first stage of research, cubic-shape samples were used to evaluation of corrosion resistance in 0.1M Na_2SO_4 solution during two corrosion tests: (i) immersion test in the time of 24 h,

[1] SILESIAN UNIVERSITY OF TECHNOLOGY, DEPARTMENT OF ADVANCED MATERIALS AND TECHNOLOGIES, 8 KRASIŃSKIEGO STR., 40-019 KATOWICE, POLAND
[2] BGH POLSKA SP. Z O.O., ŻELAZNA 9, 40-851 KATOWICE, POLAND

* Corresponding author: Maria.Sozanska@polsl.pl

72 h, 168 h and 336 h (OCP – Open Circuit Potential) and (ii) corrosion test under cathodic polarization conditions (current density 50 mA/cm^2).

In the second stage of research, the samples for SCC tests were turned from the bars (the gauge length: 20 mm, the gauge diameter: 5 mm). To evaluate the susceptibility for SCC, the slow strain rate tests (SSRT) were carried out (Standard ASTM G129 (2006): "*Standard Practice Slow Strain Rate Testing to Evaluate the Susceptibility of Metallic Materials to Environmentally Assisted Cracking*"). The strain rate ($\dot{\varepsilon}$) was set as $9 \cdot 10^{-7}$ s^{-1} and the SSRT was performed in four variants: (i) in air; (ii) in air after 24 h of immersion in 0.1M Na_2SO_4 solution; (iii) in 0.1M Na_2SO_4 solution in OCP conditions; (iv) in 0.1M Na_2SO_4 solution during *in situ* hydrogenation under conditions of cathodic polarization (current density 50 mA/cm^2). The corrosion products after SSRT were removed from the fractures by the solution containing CrO_3 (200 g/dm^3) and $AgNO_3$ (10 g/dm^3). Then the fractures were rinsed in acetone using ultrasonic cleaner. The microstructure of samples were investigated by scanning electron microscope (SEM) Hitachi S-3400N equipped with energy dispersive X-ray spectrometer (EDS) Thermo Noran. The analysis of phase composition was performed by JEOL JDX-7S X-ray diffractometer.

3. Results and discussion

Morphology, chemical and phase composition of corrosion products (without mechanical loads)

As a result of immersion of the samples in the 0.1M Na_2SO_4 solution (OCP conditions), typical corrosion changes were observed. After 24 h of exposure to the corrosive environment, the formation of local areas affected by corrosion changes of the α-Mg matrix was observed (Fig. 1a). After 72 h of immersion, the areas of the corrosion covered almost the entire surface of the sample (Fig. 1b). After 168 h of immersion, areas affected by corrosion changes merged to form a continuous layer of corrosion products, covering the entire surface of the sample (Fig. 1c). After 336 h of exposure, the entire surface of the sample was still covered with a continuous layer of corrosion products (Fig. 1d). It should be noted that the corrosion products formed on the surface of the immersed samples were characterized by the large number of cracks. Nevertheless, no signs of scaling of corrosion products from samples were observed, regardless of the time of their exposure to the corrosive environment.

Observations of the surface layer of the samples on cross-sections (Fig. 2) showed that with the increase of exposure time of the AE44 alloy to Na_2SO_4 solution, the range of corrosion changes into the material also increased. After 24 h (Fig. 2a), the average thickness of corrosion layer was 4.0 ± 1.4 µm. After 72 h (Fig. 2b), the average thickness of corrosion products increased to 6.4 ± 1.0 µm, while after 168 h (Fig. 2c) – to 13.4 ± 2.7 µm. After 336 h (Fig. 2d), the average thickness of corrosion layer into the alloy reached 34.3 ± 5.8 µm. It shows that the layer of corrosion products formed on the alloy surface provides only partial protection against corrosive environment. It may be caused by the numerous cracks in the layer which facilitate the contact of the environment with metallic substrate.

Analysis of the chemical composition (EDS) of corrosion layer on the AE44 alloy after immersion in Na_2SO_4 solution showed that its main components are: magnesium, oxygen, aluminum, lanthanum, cerium, manganese and sulfur (Fig. 3).

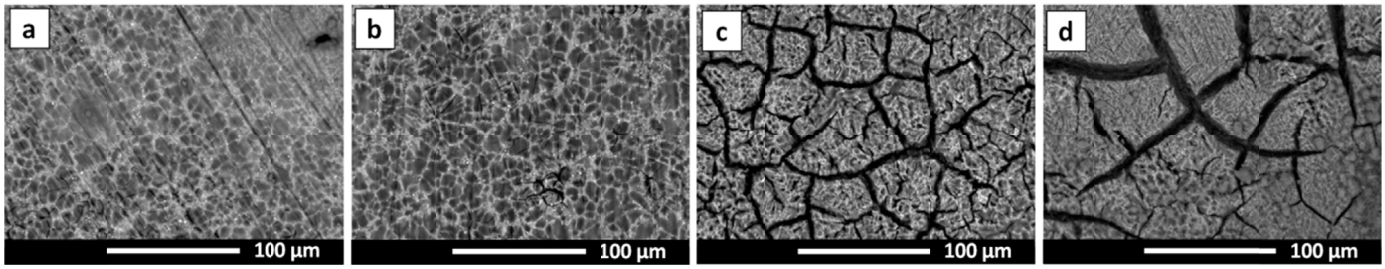

Fig. 1. Microstructure of the samples made of AE44 alloy after corrosion test in OCP conditions (0.1M Na_2SO_4 solution): (a) 24 h; (b) 72 h; (c) 168 h; (d) 336 h of immersion

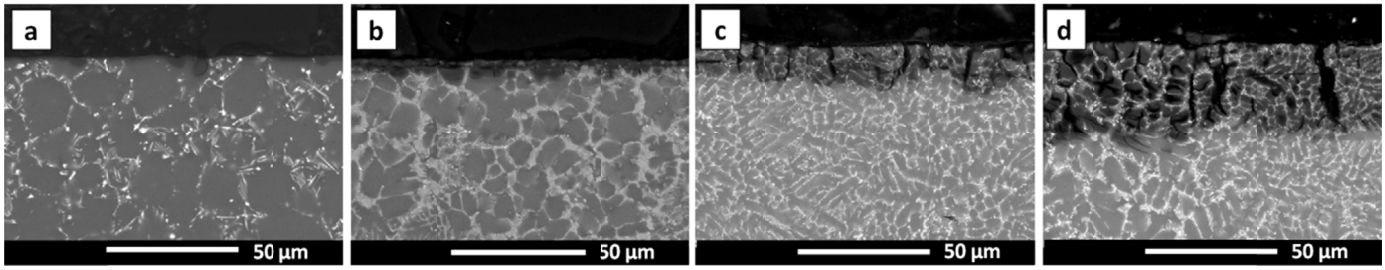

Fig. 2. Microstructure of cross-sections of samples made of AE44 alloy after corrosion test in the OCP conditions (0.1M Na_2SO_4 solution): (a) 24 h; (b) 72 h; (c) 168 h; (d) 336 h of immersion

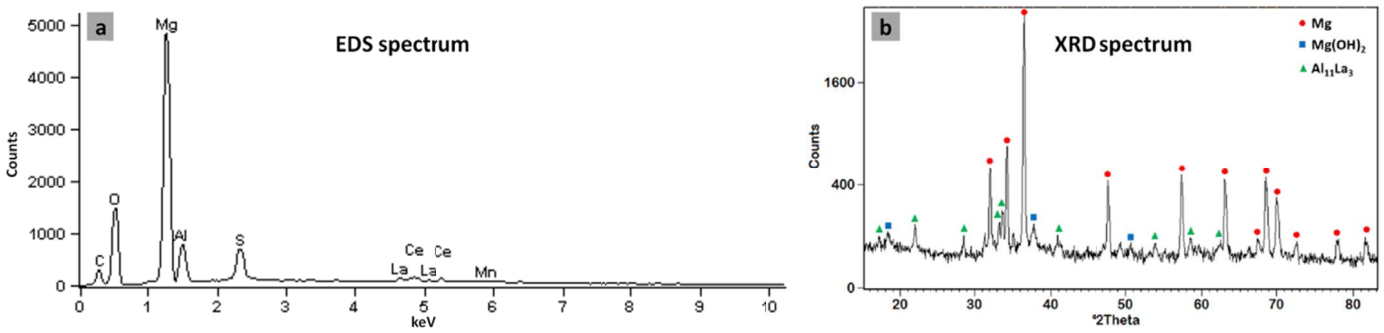

Fig. 3. Results of analysis of chemical composition (EDS) and phase composition (XRD) of corrosion layer on AE44 magnesium alloy

Analysis of the phase composition of the AE44 alloy after 168 h of exposure to Na_2SO_4 solution showed that the surface layer of the sample consisted of α-Mg (matrix), $Mg(OH)_2$ and $Al_{11}La_3$ phase (Fig. 3).

On the surface of the AE44 alloy after exposure to the 0.1M Na_2SO_4 solution in the cathodic polarization conditions, gradual formation of the corrosion layer on the samples was observed (Fig. 4). The number and size of areas changed by corrosion did not change significantly as the exposure time increased, what confirm good corrosion resistance of this alloy.

Observations on cross sections confirmed the presence of a layer formed on the surface of the alloy (Fig. 5) after 8 h of exposure (Fig. 5d). The average thickness of the layer was 0.7 ± 0.3 µm. With the increase of time, the thickness of the layer formed on the surface slightly increased. After 16 h of exposure (Fig. 5e) the thickness increased to 1.1 ± 0.2 µm, whereas after 24 h of exposure (Fig. 5f) – up to 1.5 ± 0.2 µm.

Morphology of fracture surface in conditions stress corrosion cracking (SSC)

Stress-strain curves obtained as a result of four variants of SSRT are shown in Fig. 6. The obtained curves are typical, with zones of elastic and plastic deformation, but without a physical yield point. Therefore, the proof stress $R_{p0.2}$ was determined, whose value regardless of the variant of the SSRT was similar and amounted to about 100 MPa. In the case of one of the samples deformed in the air (Fig. 6 – AE44-I-1), this value was slightly higher and amounted to 110 MPa. The highest tensile strength ($R_m \approx 170$ MPa) was found in case of samples deformed in the air. Slightly lower strength ($R_m \approx 140$ MPa) was found for the samples deformed in air after immersion in Na_2SO_4 solution and samples deformed in the Na_2SO_4 solution under OCP conditions ($R_m \approx 150$ MPa). The lowest strength ($R_m \approx 110$ MPa) reveal the samples deformed in solution under cathodic polarization conditions. The change in elongation was very significant: samples

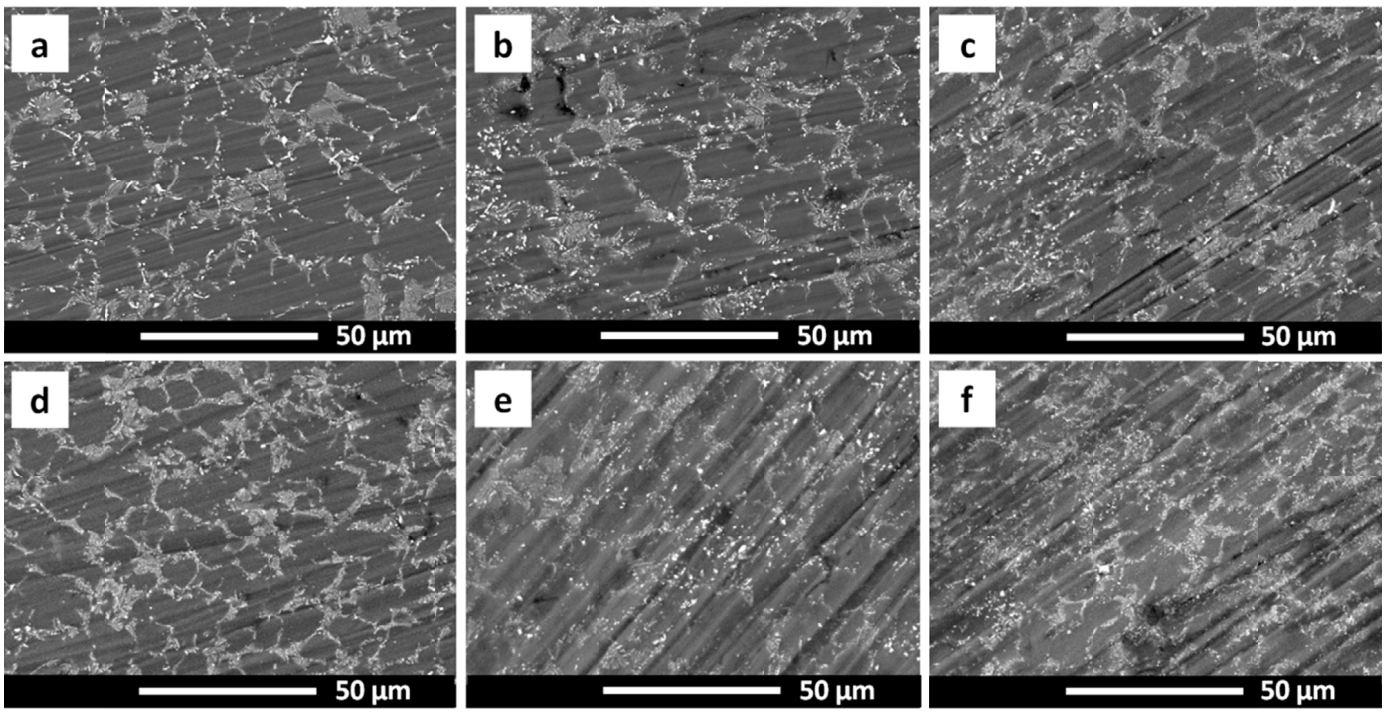

Fig. 4. Microstructure of the samples made of AE44 alloy after corrosion test in cathodic polarization conditions (0.1M Na_2SO_4 solution): (a) before test; (b) 2 h; (c) 4 h; (d) 8 h; (e) 16 h; (f) 24 h

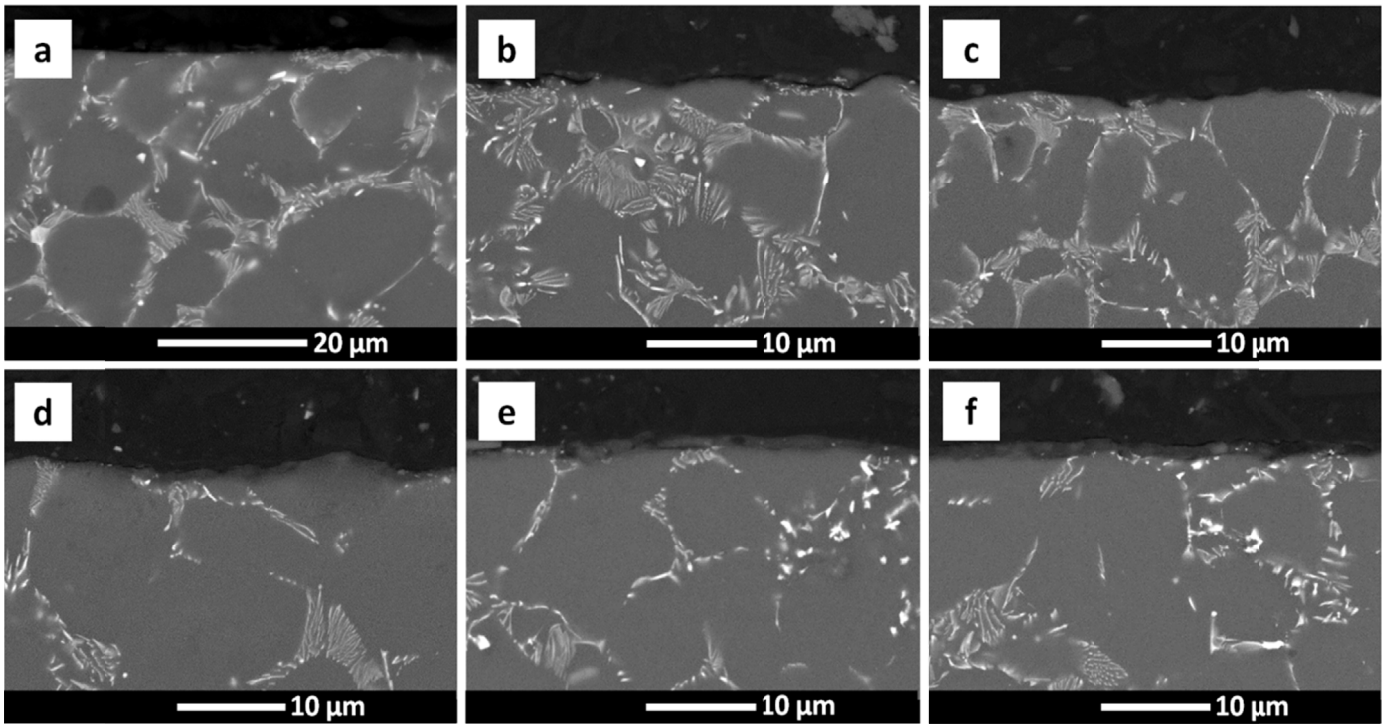

Fig. 5. Microstructure of cross-sections of samples made of AE44 alloy after corrosion test in cathodic polarization conditions (0.1M Na_2SO_4 solution): (a) before test; (b) 2 h; (c) 4 h; (d) 8 h; (e) 16 h; (e) 24 h

deformed in air after immersion in solution were characterized by the elongation lower about 34÷39% in comparison to samples deformed in solution (OCP conditions). This unexpected result seems to confirm that AE44 alloy is less susceptible to SCC in OCP conditions than in air after immersion in corrosive solution.

Investigation of the fractures after SSRT reveals some pores with varying sizes (Fig. 7). This porosity was created during the die-casting of the AE44 alloy and it is typical for this process. The presence of many cracks on the fractures was also found (Fig. 7).

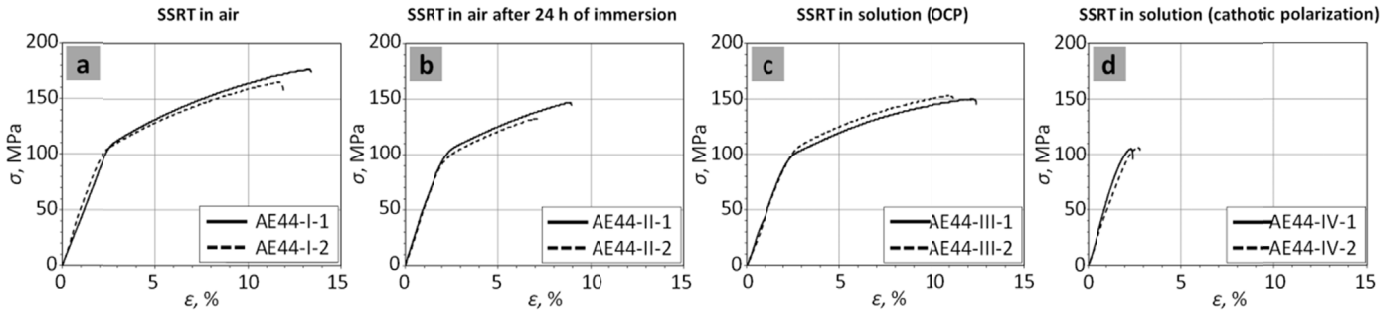

Fig. 6. Stress-strain curves ($\dot{\varepsilon} = 9 \cdot 10^{-7}$ s^{-1}) for the samples made of AE44 alloy after SSRT in air, in air after immersion in Na_2SO_4 solution, in Na_2SO_4 solution (OCP) and in Na_2SO_4 solution (cathodic polarization)

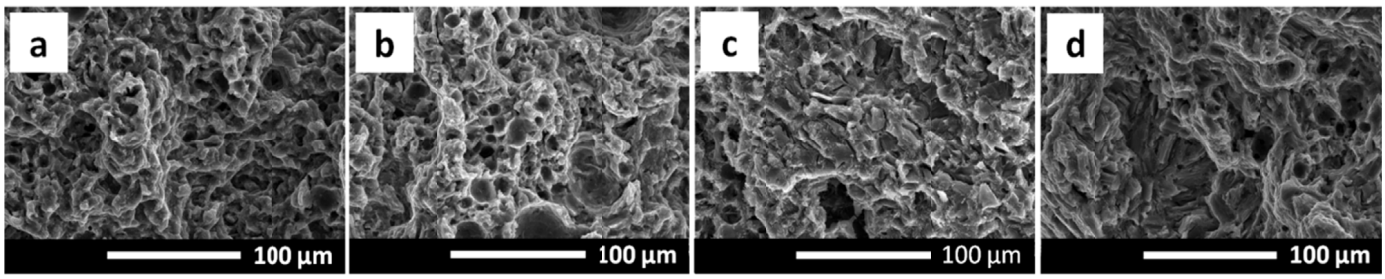

Fig. 7. Typical fracture images of AE44 alloy: (a) SSRT in air; (b) SSRT in air after immersion in Na_2SO_4 solution; (c) SSRT in Na_2SO_4 solution (OCP); (d) SSRT in Na_2SO_4 solution (cathodic polarization)

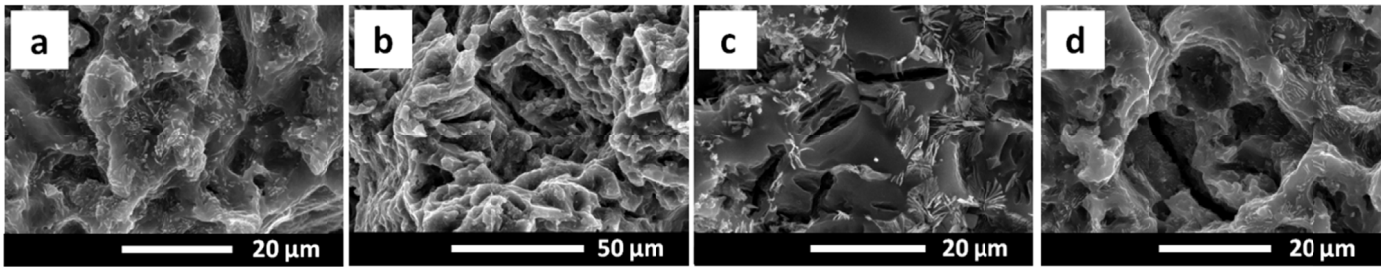

Fig. 8. Characteristic details fracture of AE44 alloy: (a) SSRT in air; (b) SSRT in air after immersion in Na_2SO_4 solution; (c) SSRT in Na_2SO_4 solution (OCP); (d) SSRT in Na_2SO_4 solution (cathodic polarization)

The detailed analysis of the fractures morphology (Fig. 8) showed that:

- SSRT in the air leads to the intergranular fractures with few small micro cracks;
- SSRT in air (after immersion in Na_2SO_4 solution) or in solution (OCP and cathodic polarization conditions) leads to transgranular fractures with brittle areas and many micro cracks;
- the microcracks of the fractures were mainly transgranular, but there were also rare intergranular cracks;
- secondary cracks visible on the fractures were small and were located only close to surface of the samples.

4. Summary

In the summary of electrochemical corrosion results (two corrosion tests: (i) immersion test in the time of 24 h, 72 h, 168 h and 336 h (OCP – Open Circuit Potential) and (ii) corrosion test under cathodic polarization conditions (current density 50 mA/cm^2) and stress corrosion cracking (SSC) (four variants SSRT: (i) in air; (ii) in air after 24 h of immersion in 0.1M Na_2SO_4 solution; (iii) in 0.1M Na_2SO_4 solution in OCP conditions; (iv) in 0.1M Na_2SO_4 solution during *in situ* hydrogenation under conditions of cathodic polarization (current density 50 mA/cm^2)) and of the qualitative evaluation of fracture surfaces after the SSRT tests, the following conclusions were formulated for AE44 alloy:

1. Analysis of corrosion products on the AE44 alloy in the 0.1M Na_2SO_4 solution (OCP conditions) in OCP conditions and under cathodic polarization conditions (current density 50 mA/cm^2) showed that:
   – in OCP conditions with increasing immersion time of the samples in the solution (from 24 h to 336 h), the corrosion products (locally on the surface after 24h to almost total surface coverage after 72 hours) were observed with a characteristic network of cracks reaching up to the metallic alloy matrix, and under cathodic polarization conditions gradual formation of the corrosion layer on the samples was observed, and the number and size of areas changed by corrosion did not change significantly as the exposure time increased,
   – in OCP conditions – the thickness of corrosion products has changed since 4.0 µm after 24 h, to 6.4 µm after 72 h, 13.4 µm after 168 h and 34.3 µm after 336 h, a under cathodic polarization conditions – 0.7 µm after 8 h, 1.1 µm after 16 h i 1.5 µm after 24 h,
   – analysis of chemical and phase composition showed that the corrosion products contained mainly: magnesium, oxygen, aluminum, lanthanum, cerium, manganese and sulfur, and in terms of phase composition: α-Mg (matrix), $Mg(OH)_2$ and $Al_{11}La_3$ phase.
2. The impact of mechanical loads and the corrosive environment (in three variants SSRT) under stress corrosion cracking SSC conditions on the properties of AE44 took the form of deterioration in mechanical properties with different levels depending on the test condition.
3. The qualitative fractography analysis of the fracture surfaces of the AE44 specimens after the SSR tests in air and in the corrosive solution under three variants conditions revealed intergranular fractures with few small microcracks in air and transgranular fractures with brittle areas and many microcracks in the case of the specimens tested in the corrosive environment, the microcracks of the fractures were mainly transgranular, but there were also rare intergranular.

Acknowledgements

This work partially was supported by the National Science Centre in Poland under the research grant "Effect of hydrogen on structure and stress corrosion cracking of selected magnesium alloys from Mg-Y-RE-Zr and Mg-Al-RE systems" No. 2011/03/B/ST8/06387 and by Silesian University of Technology in grant BK-205/RM0/2019 (11/990/BK_19/0063).

REFERENCES

[1] W. Walke, E. Hadasik, J. Przondziono, D. Kuc, I. Bednarczyk, G. Niewielski, Plasticity and corrosion resistance of magnesium alloy WE43, Archives of Materials Science and Engineering **51** (1), 16-24 (2011).

[2] T. Rzychoń, J. Michalska, A. Kiełbus, Corrosion resistance of Mg-RE-Zr alloys, Journal of Achievements in Materials and Manufacturing Engineering **21** (1), 51-54 (2007).

[3] H. Ardelean, A. Seyeux, S. Zanna, F. Prima, I. Frateur, P. Marcus, Corrosion processes of Mg-Y-Nd-Zr alloys in Na2SO4 electrolyte, Corrosion Science **73**, 196-207 (2013).

[4] G.L. Song, Corrosion behavior and prevention strategies for magnesium (Mg) alloys, in: Corrosion Prevention of Magnesium Alloys: A Volume in Woodhead Publishing Series in Metals and Surface Engineering 1st Edition, 3-37 (2013).

[5] R.C. Zeng, J. Zhang, W.J. Huang, W. Dietzel, K.U. Kainer, C. Blawert, K. Wei, W. Ke, Review of studies on corrosion of magnesium alloys, Transactions of Nonferrous Metals Society of China **16**, 763-771 (2006).

[6] I. Pietkun-Greber, R. Janka, Analiza skutków oddziaływania wodoru na metale i stopy, Chemia-Dydatkyka-Ekologia-Metrologia **4** (2), 75-78 (2011) (in Polish).

[7] T. Zakroczymski, Modyfikacja powierzchni metali w celu zapobiegania korozji wodorowej, Ochrona Przed Korozją **4**, 99-102 (2006) (in Polish).

[8] T. Zakroczymski, Metody zapobiegania absorpcji wodoru przez metale, Ochrona Przed Korozją **4**, 90-93 (2005) (in Polish).

[9] I. Pietkun-Greber, R. M. Janka, Oddziaływanie wodoru na metale i stopy, Proceedings of ECOpole **4** (2), 471-476 (2010) (in Polish).

[10] A. Zieliński, Niszczenie wodorowe metali nieżelaznych i ich stopów, Gdańskie Towarzystwo Naukowe, 1999 (in Polish).

[11] J. Flis, Corrosion of metals and hydrogen-related phenomena – Selected topics 59 1st Edition, Elsevier, 1991.

[12] J. Chen, M. Ai, J. Wang, E.H. Han, W. Ke, Formation of hydrogen blister on AZ91 magnesium alloy during cathodic charging, Corrosion Science, 1197-1200 (2009).

[13] J. Chen, J. Wang, E.-H. Han, W. Ke, In situ observation of pit initiation of passivated AZ91 magnesium alloy, Corrosion Science **51**, 477–484 (2009).

[14] J. Wang, J. Chen, E. Han, W. Ke, Investigation of Stress Corrosion Cracking Behaviors of an AZ91 Magnesium Alloy in 0.1 kmol/m^3 Na_2SO_4 Solution Using Slow Strain Rate Test, Materials Transactions **49** (5), 1052-1056 (2008).

[15] J. Chen, J. Wang, E. Han, W. Ke, Electrochemical corrosion and mechanical behaviors of the charged magnesium, Materials Science and Engineering A **494**, 257-262 (2008).

[16] B. Chmiela, A. Mościcki, M. Sozańska, Investigation of Stress Corrosion Cracking in Magnesium Alloys, Solid State Phenomena **211**, 89-92 (2013).

[17] L.F. Zhou, Z.Y. Liu, W. Wu, X.G. Li, C.W. Du, B. Jiang, Stress corrosion cracking behavior of ZK60 magnesium alloy under different conditions, International Journal of Hydrogen Energy **42** (41), 26162-26174 (2017).

[18] M. Bobby Kannan, W. Dietzel, R.K.S. Raman, P. Lyon, Hydrogen-induced-cracking in magnesium alloy under cathodic polarization, Scripta Materialia **57** (7), 579-581 (2007).

[19] A. Mościcki, B. Chmiela, M. Sozańska, J. Łabanowski, Wpływ jednoczesnego oddziaływania obciążeń mechanicznych oraz środowiska zawierającego wodór na właściwości stopu WE43 – krótkie doniesienie, Ochrona Przed Korozją **58** (5), 203, (2015).

[20] A. Atrens, N. Winzer, W. Dietzel, P.. Srinivasan, G.-L. Song, Stress corrosion cracking (SCC) of magnesium (Mg) alloys, in: Corrosion of Magnesium Alloys, Elsevier, 299-364 (2011).

[21] N. Winzer, A. Atrens, G. Song, E. Ghali, W. Dietzel, K.U. Kainer, N. Hort, C. Blawert, A Critical Review of the Stress Corrosion Cracking (SCC) of Magnesium Alloys, Advanced Engineering Materials **7** (8), 659-693 (2005).

[22] A. Atrens, N. Winzer, W. Dietzel, P.. Srinivasan, G.-L. Song, Stress corrosion cracking(SCC) of magnesium (Mg) alloys, in: Corrosion of Magnesium Alloys, Elsevier, 299-364 (2011).

[23] M. Bobby Kannan, W. Dietzel, C. Blawert, A. Atrens, P. Lyon, Stress corrosion cracking of rare-earth containing magnesium alloys ZE41, QE22 and Elektron 21 (EV31A) compared with AZ80, Materials Science and Engineering A **480** (1-2), 529-539. (2008).

[24] B.S. Padekar, R.K. Singh Raman, V.S. Raja, L. Paul, Stress corrosion cracking of a recent rare-earth containing magnesium alloy, EV31A, and a common Al-containing alloy, AZ91E, Corrosion Science **71**, 1-9 (2013).

[25] L. Choudhary, R.K. Singh Raman, J. Hofstetter, P.J. Uggowitzer, In-vitro characterization of stress corrosion cracking of aluminium-free magnesium alloys for temporary bio-implant applications, Materials Science and Engineering C **42**, 629-636 (2014).

[26] M. Sozańska, A. Mościcki, B. Chmiela, Investigation of Stress Corrosion Cracking in Magnesium Alloys by Quantitative Fractography Methods, Archives of Metallurgy and Materials **62**, 557-562 (2017).